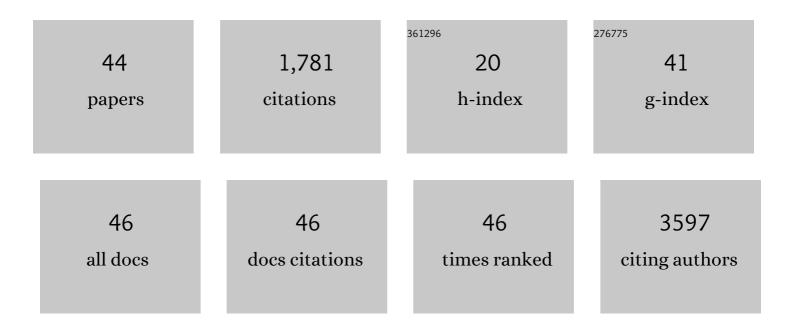
## Mengkun Tian

List of Publications by Year in descending order

Source: https://exaly.com/author-pdf/8517411/publications.pdf Version: 2024-02-01



#	Article	IF	CITATIONS
1	Interlayer Coupling in Twisted WSe <sub>2</sub> /WS <sub>2</sub> Bilayer Heterostructures Revealed by Optical Spectroscopy. ACS Nano, 2016, 10, 6612-6622.	7.3	249
2	Structure and Formation Mechanism of Black TiO <sub>2</sub> Nanoparticles. ACS Nano, 2015, 9, 10482-10488.	7.3	170
3	Controlling the Surface Oxidation of Cu Nanowires Improves Their Catalytic Selectivity and Stability toward C <sub>2+</sub> Products in CO <sub>2</sub> Reduction. Angewandte Chemie - International Edition, 2021, 60, 1909-1915.	7.2	122
4	Tailoring Vacancies Far Beyond Intrinsic Levels Changes the Carrier Type and Optical Response in Monolayer MoSe <sub>2â~<i>x</i></sub> Crystals. Nano Letters, 2016, 16, 5213-5220.	4.5	121
5	Pulsed Laser Deposition of Photoresponsive Twoâ€Dimensional GaSe Nanosheet Networks. Advanced Functional Materials, 2014, 24, 6365-6371.	7.8	108
6	A safe and fast-charging lithium-ion battery anode using MXene supported Li <sub>3</sub> VO <sub>4</sub> . Journal of Materials Chemistry A, 2019, 7, 11250-11256.	5.2	106
7	Ultrafast Charge Transfer and Hybrid Exciton Formation in 2D/0D Heterostructures. Journal of the American Chemical Society, 2016, 138, 14713-14719.	6.6	102
8	Deeply Rechargeable and Hydrogen-Evolution-Suppressing Zinc Anode in Alkaline Aqueous Electrolyte. Nano Letters, 2020, 20, 4700-4707.	4.5	89
9	Suppression of Defects and Deep Levels Using Isoelectronic Tungsten Substitution in Monolayer MoSe <sub>2</sub> . Advanced Functional Materials, 2017, 27, 1603850.	7.8	84
10	Tandem laser ablation synthesis in solution-galvanic replacement reaction (LASiS-GRR) for the production of PtCo nanoalloys as oxygen reduction electrocatalysts. Journal of Power Sources, 2016, 306, 413-423.	4.0	63
11	Ultrafine Pd ensembles anchored-Au2Cu aerogels boost ethanol electrooxidation. Nano Energy, 2018, 53, 206-212.	8.2	54
12	The Effect of Nickel on MoS <sub>2</sub> Growth Revealed with <i>in Situ</i> Transmission Electron Microscopy. ACS Nano, 2019, 13, 7117-7126.	7.3	48
13	Digital Transfer Growth of Patterned 2D Metal Chalcogenides by Confined Nanoparticle Evaporation. ACS Nano, 2014, 8, 11567-11575.	7.3	47
14	Strain tolerance of two-dimensional crystal growth on curved surfaces. Science Advances, 2019, 5, eaav4028.	4.7	46
15	Defect-Mediated Alloying of Monolayer Transition-Metal Dichalcogenides. ACS Nano, 2018, 12, 12795-12804.	7.3	42
16	Hybrid nanocomposites of nanostructured Co <sub>3</sub> O <sub>4</sub> interfaced with reduced/nitrogen-doped graphene oxides for selective improvements in electrocatalytic and/or supercapacitive properties. RSC Advances, 2017, 7, 33166-33176.	1.7	41
17	Nonequilibrium Synthesis of TiO <sub>2</sub> Nanoparticle "Building Blocks―for Crystal Growth by Sequential Attachment in Pulsed Laser Deposition. Nano Letters, 2017, 17, 4624-4633.	4.5	33
18	Synthetic Engineering of Morphology and Electronic Band Gap in Lateral Heterostructures of Monolayer Transition Metal Dichalcogenides. ACS Nano, 2020, 14, 6323-6330.	7.3	24

Mengkun Tian

#	Article	IF	CITATIONS
19	Bottom up synthesis of boron-doped graphene for stable intermediate temperature fuel cell electrodes. Carbon, 2017, 123, 605-615.	5.4	23
20	Antiferroelectric negative capacitance from a structural phase transition in zirconia. Nature Communications, 2022, 13, 1228.	5.8	22
21	Effect of morphology on anion conductive properties in self-assembled polystyrene-based copolymer membranes. Journal of Membrane Science, 2018, 565, 213-225.	4.1	19
22	The ion and water transport properties of K+ and Na+ form perfluorosulfonic acid polymer. Electrochimica Acta, 2018, 282, 544-554.	2.6	19
23	On the Role of Li <sup>+</sup> Codoping in Simultaneous Improvement of Light Yield, Decay Time, and Afterglow of Lu <sub>2</sub> SiO <sub>5</sub> :Ce <sup>3+</sup> Scintillation Detectors. Physica Status Solidi - Rapid Research Letters, 2019, 13, 1800472.	1.2	16
24	In Situ Dynamics during Heating of Copper-Intercalated Bismuth Telluride. Matter, 2020, 3, 1246-1262.	5.0	16
25	Black Anatase Formation by Annealing of Amorphous Nanoparticles and the Role of the Ti <sub>2</sub> O <sub>3</sub> Shell in Self-Organized Crystallization by Particle Attachment. ACS Applied Materials & Interfaces, 2017, 9, 22018-22025.	4.0	15
26	Recent progress in characterization of the core–shell structure of black titania. Journal of Materials Research, 2019, 34, 1138-1153.	1.2	15
27	Controlling the Surface Oxidation of Cu Nanowires Improves Their Catalytic Selectivity and Stability toward C 2+ Products in CO 2 Reduction. Angewandte Chemie, 2021, 133, 1937-1943.	1.6	13
28	Nanostructured carbon electrocatalyst supports for intermediate-temperature fuel cells: Single-walled versus multi-walled structures. Journal of Power Sources, 2017, 337, 145-151.	4.0	12
29	High-temperature transformation of Fe-decorated single-wall carbon nanohorns to nanooysters: a combined experimental and theoretical study. Nanoscale, 2013, 5, 1849-1857.	2.8	10
30	A Janovecâ€Kayâ€Dunnâ€Like Behavior at Thickness Scaling in Ultraâ€Thin Antiferroelectric ZrO <sub>2</sub> Films. Advanced Electronic Materials, 2021, 7, 2100485.	2.6	8
31	Surface Mechanoengineering of a Zr-Based Bulk Metallic Glass via Ar-Nanobubble Doping To Probe Cell Sensitivity to Rigid Materials. ACS Applied Materials & Interfaces, 2017, 9, 43429-43437.	4.0	7
32	Measuring the areal density of nanomaterials by electron energy-loss spectroscopy. Ultramicroscopy, 2019, 196, 154-160.	0.8	7
33	Polymer-Ligated Uniform Lead Chalcogenide Nanoparticles with Tunable Size and Robust Stability Enabled by Judiciously Designed Surface Chemistry. Chemistry of Materials, 2021, 33, 6701-6712.	3.2	6
34	Self-assembled <sup>nat</sup> LiCl–CeCl <sub>3</sub> directionally solidified eutectics for thermal neutron detection. CrystEngComm, 2020, 22, 3269-3273.	1.3	5
35	Characterization of diamond films deposited on Re substrate by magnetic field-assisted hot filament chemical vapor deposition. Applied Surface Science, 2012, 258, 2117-2120.	3.1	4
36	Diamond film growth on the Mo–Re alloy foil. Journal of Crystal Growth, 2011, 314, 58-61.	0.7	3

Mengkun Tian

#	Article	IF	Citations
37	Transition Metal Dichalcogenides: Suppression of Defects and Deep Levels Using Isoelectronic Tungsten Substitution in Monolayer MoSe <sub>2</sub> (Adv. Funct. Mater. 19/2017). Advanced Functional Materials, 2017, 27, .	7.8	3
38	H <sub>2</sub> O-prompted CO <sub>2</sub> capture on metal silicates <i>in situ</i> generated from SBA-15. RSC Advances, 2020, 10, 28731-28740.	1.7	3
39	Detection of plasmonic behavior in colloidal indium tin oxide films by impedance spectroscopy. MRS Communications, 2020, 10, 278-285.	0.8	3
40	Nanocrystalline Diamond Matrix Deposited on Copper Substrate by Radical Species Restricted Diffusion. Journal of Nanoscience and Nanotechnology, 2013, 13, 6910-6916.	0.9	2
41	Laser Synthesis, Processing, and Spectroscopy of Atomically-Thin Two Dimensional Materials. Springer Series in Materials Science, 2018, , 1-37.	0.4	1
42	Mapping Giant Oscillator Excitons in Semiconducting Nano Wires. Microscopy and Microanalysis, 2017, 23, 374-375.	0.2	0
43	Structures of Boron Loaded Turbostratic Graphene with Enhanced Performance in Solid Acid Fuel Cell. ECS Meeting Abstracts, 2017, , .	0.0	Ο
44	Influence of Metal Dopants on MoS2 Crystallization Investigated through in Situ Electron Microscopy. ECS Meeting Abstracts, 2019, , .	0.0	0